Numerical Investigation of the Axially Compressive Behavior of Circular Concrete Encased Steel Composite (CESC) Columns

Hoang An Le
Ho Chi Minh City University of Transport, Vietnam
hoangan.le@ut.edu.vn
(corresponding author)

Received: 29 December 2022 | Revised: 5 February 2023 | Accepted: 8 February 2023

ABSTRACT

This research presents a numerical investigation of circular Concrete Encased Steel Composite (CESC) columns. To simulate the circular CESC columns under axial compression in the previous tests, a Finite Element Model (FEM) with some modifications of material models for the steel and concrete was established in ABAQUS software. The curves of load versus longitudinal displacement and the ultimate loads obtained from the FEM were compared with those measured in previous tests. The numerical results agreed well with the test results. Furthermore, the distribution of the stresses on the cross-section at different heights and the effect of initial imperfections were observed by the FEM results. A highly confined concrete zone enclosed by steel web and steel flanges was observed. Finally, the established FEM was used in the parametric study that investigated the influence of concrete strength, steel yield strength, and spacing of the spiral hoops.

Keywords-composite columns; FEM; CES; ABAQUS; concrete; steel

I. INTRODUCTION

Concrete Encased Steel Composite (CESC) columns are being widely applied in heavy-loading structures such as in top-down construction methods, high-rise buildings, or support structures [1, 3-4, 24-28]. The utilization of circular CESC columns in construction was found to be necessary due to their ability to support higher loads than the rectangular or square CESC columns and their aesthetical appearance. A steel section is constructed inside the reinforced concrete to form a CESC column, thereby fully exploiting the advantages of steel and concrete materials [1, 24-26]. Ductility and seismic resistance can be greatly enhanced by the use of a steel section, while the concrete works as a protective layer for the steel section against buckling, fire, and aggressive environments [1-2, 8, 19, 28-30]. For these reasons, several attempts have been made to test the structural behavior of CESC columns [1-5, 8, 13-14, 24, 27, 29-30].

The testing equipment for CESC columns requires very high capacity and complexity, thus restricting the range of parameters. Therefore, many efforts have been undertaken to simulate the behavior of CESC columns through Finite Element Models (FEMs). Authors in [4] presented a FEM to analyze the pin-ended axially loaded square CESC short and long columns using various concrete strengths (20-110MPa) and various steel yield strengths (275-690MPa). Authors in [11] introduced a new simplified technique of FEM incorporating the confinement effect of square CESC columns to construct strength interaction diagrams. Authors in [7] constructed FEMs to compare the difference between square CESC columns and reinforced concrete columns with different concrete strengths. Authors in [15] constructed a FEM to study the buckling resistance of CESC columns using concrete strength up to 100MPa. Authors in [9] conducted simulations to address the impact of concrete strength, steel strength, and column slenderness on the performance of square CESC columns. Authors in [10] simulated a square CESC long column with 3.6m length and a steel column made of welded H-profile with the same length under axial compression and uniaxial bending to compare the difference between CESC and pure steel columns. Authors in [12] constructed a FEM of square CESC columns using Fiber-Reinforced Concrete (FRC) to verify the test results and the effect of tensile strength of FRC.

The literature review revealed that the majority of existing numerical investigations of the behavior of CESC columns were concerned with square sections, while the studies on CESC columns with circular sections are extremely limited. As compared to square or rectangular sections with the same dimensions, the use of circular sections results in some beneficial characteristics for CESC columns such as higher confining stress induced by steel profile and transverse reinforcements, higher strength and ductility, and better

architectural performance [5, 7, 18, 20]. Only two test results of circular CESC columns were reported in [7]. For this reason, there is a need for the study of circular CESC columns, in general, and FEM studies for circular CESC columns, in particular. To fulfill this gap, this paper presents a FEM to simulate the circular CESC short columns. Firstly, the FEM was established in ABAQUS software with some modifications to material models. After this, the accuracy of the FEM was checked by comparing it with the test results of [7]. The distribution of stresses on the cross-section at different heights was also plotted. Finally, the effect of the concrete strength, steel yield strength, and spacing of spiral hoops on the load versus displacement response of circular CESC short columns was determined by conducting a parametric study.

II. DESCRIPTION OF FEM

A. Configuration of Test Specimens

Test specimens reported in [7] were used for the simulation. Two circular CESC short columns using an I cross-shaped steel section were constructed for testing under concentric loading. Table I shows the geometry and the dimensions of the columns and Table II demonstrates the properties of the materials used for the test specimens.

TABLE I. DIMENSIONS OF TEST SPECIMENS

Specimens	Diameter (mm)	Height (mm)	Steel section
HSRC-SP1	411	1233	2H206×120×12×12
HSRC-SP2	411	1233	2H206×120×12×12

Specimens	Longitudinal reinforcement	Spiral hoop	Spacing of spiral hoop (mm)	Ultimate load (kN)
HSRC-SP1	20d10	d10	50	11363
HSRC-SP2	20d10	d10	50	10890

TABLE II. MATERIAL PROPERTIES OF TEST SPECIMENS

Specimens	Concrete strength f_c (MPa)	Yield strength of steel section f_y (MPa)	Yield strength of longitudinal reinforcement $f_{y,r}$ (MPa)	Yield strength of spiral hoop $f_{h,h}$ (MPa)
HSRC-SP1	37	517	426	426
HSRC-SP2	37	517	426	426

B. Mesh and Finite Elements

The circular CESC columns consisted of concrete, steel section, longitudinal reinforcements, and spiral hoops. The solid element C3D8R (8-node brick element) was selected for simulating the concrete and the embedded steel profile. The truss element T3D2 (2-node) was selected to simulate the embedded longitudinal reinforcements, while the B31 beam element was adopted for modeling the spiral hoops. After the performance of different mesh sizes, a reasonable aspect ratio of solid element size of 1:3 was assumed. A coefficient of friction of 0.25 [4] was chosen in the "surface-to-surface contact" to simulate the interface of the concrete and the steel profile. It should be noted that this friction coefficient is adopted by numerous studies. Master and slave surfaces were assigned to the concrete and the encased steel section, respectively. Figure 1 shows the finite element mesh and type.

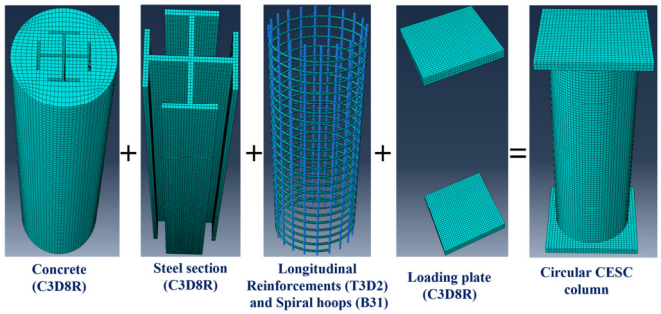

Fig. 1. Finite element mesh and type

C. Boundary Conditions and Loading Application

Two loading plates were simulated at both ends of the column and tied to the end surface of the concrete and steel section to ensure a uniform load transfer to the whole section of the column. Two reference points (RP1 and RP2) were located in the middle of the upper and lower loading plates, respectively. A rigid body constraint was assigned between the reference point and the surface of the loading plate for easier loading application. All degrees of freedom of loading plates were fixed, while the axial displacement of the upper loading plate was set free to permit the axial movement. The numerical analysis in ABAQUS [21] was carried out using displacement control. An implicit procedure with the Newton-Raphson method [21] was adopted for the analysis. Figure 2 demonstrates the modeling of boundary conditions, the interaction between structural steels and concrete, and the loading application.

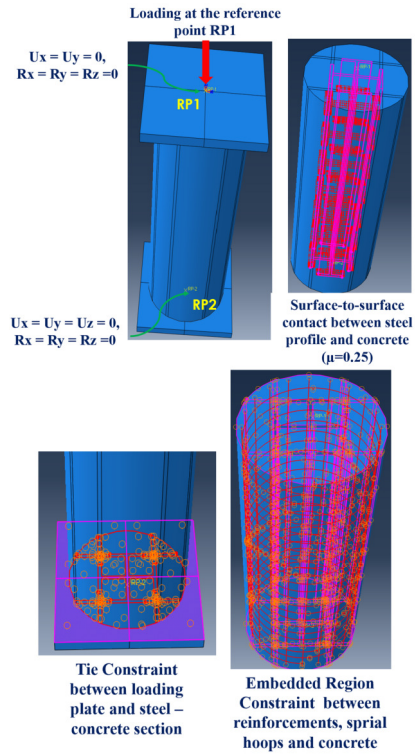

Fig. 2. Boundary condition and loading application.

The buckling mode was determined by eigenvalue buckling analysis of the simulated columns. The eigenmode 1 as the first buckling mode was adopted to incorporate the geometric initial imperfection for nonlinear inelastic analysis of the composite column. The value of the initial imperfection for each column was selected as *L*/500 and *L*/1000, in which *L* is defined as the column length.

D. Material Models

The behavior of structural steels (steel section, longitudinal reinforcement, and spiral hoop) was simulated using the stress-strain model [22] as seen in Figure 3. The value of Poisson's ratio was set as 0.3 for steel. In Figure 3, f_y represents the yield stress and ε_y denotes the strain at f_y. The modulus E_1 was taken as $0.01E_y$, while the modulus of elasticity E_y of the first elastic stage was set as 200GPa.

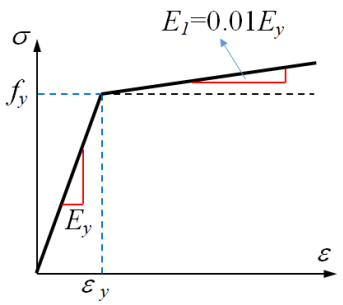

Fig. 3. Stress-strain model for structural steels.

The nonlinearity of the concrete was simulated using the Concrete Damage Plasticity Model (CDPM). Some parameters of CDPM employed to model the triaxial stress state of the concrete are:

- Angle of dilation φ=30°.
- Eccentricity ε=0.1.
- Ratio of f_{bo}/f_c=1.16, where f_{bo} is the biaxial compressive yield stress.
- Ratio of the second stress invariant on the tensile meridian for the yield function K=0.667.

Furthermore, the viscosity parameter μ=0.0001 was used to ensure the convergence. The CEB model [23] was adopted to estimate the curve of stress versus strain (σ_c-ε) of the concrete. The CEB model [23] is applicable to various concrete strengths (10-100MPa). The (σ_c-ε) curves can be drawn using the equations of the CEB model [23]:

$$\sigma_c = f_c \left[\frac{\left(\frac{E_{it}}{E_0}\right)\left(\frac{\varepsilon}{\varepsilon_0}\right) - \left(\frac{\varepsilon}{\varepsilon_0}\right)^2}{1 + \left(\frac{E_{it}}{E_0} - 2\right)\left(\frac{\varepsilon}{\varepsilon_0}\right)} \right] \quad \text{For } \varepsilon \le \varepsilon_0 \qquad (1)$$

$$\varepsilon_0 = 0.7(f_c)^{0.31} \times 10^{-3} \qquad (2)$$

$$E_{it} = 22000(f_c/10)^{0.3} \qquad (3)$$

$$\sigma_c = \frac{f_c}{1 + \left(\frac{\frac{\varepsilon}{\varepsilon_0} - 1}{\eta - 1}\right)^2} \quad \text{for } \varepsilon > \varepsilon_0 \qquad (4)$$

$$\eta = (\varepsilon_0 + 0.001)/\varepsilon_0 \qquad (5)$$

where ε_0 is the longitudinal strain at f_c, E_0 is defined as the secant modulus at f_c, and E_{it} is the tangent modulus.

The curve of stress versus plastic strain of concrete (f_c = 37MPa) for the test specimens in [7] used as input in ABAQUS is shown in Figure 4.

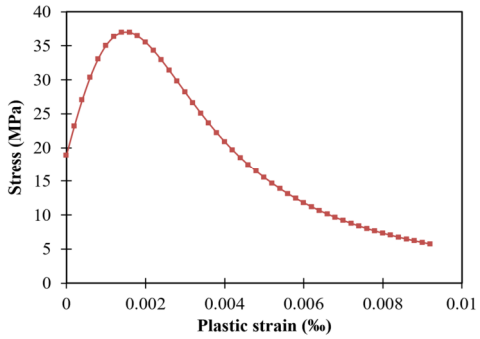

Fig. 4. Stress – plastic strain relation of concrete.

III. FEM VALIDATION

The load versus displacement (*L-D*) curve and the ultimate load obtained from FEM were compared with those measured in the tests conducted in [7] to evaluate the suitability of the FEM. Figure 5 shows the *L-D* curves of the FEM and the test results of [7]. It can be seen that the *L-D* curves from the FEM matched well with the test results. Furthermore, the FEM *L-D* curves of FEM with and without imperfections were plotted. Figure 5 shows that there is no significant change in the *L-D* curves with and without initial imperfections in FEM. The ultimate loads measured in the tests (N_{Test}) and FEM (N_{FEM1} and N_{FEM2}) are compared in Table III. It is evident that the ultimate loads of FEM are close to those obtained from the tests in [7] with FEM underestimating the ultimate loads with a difference ranging from 5% to 9%.

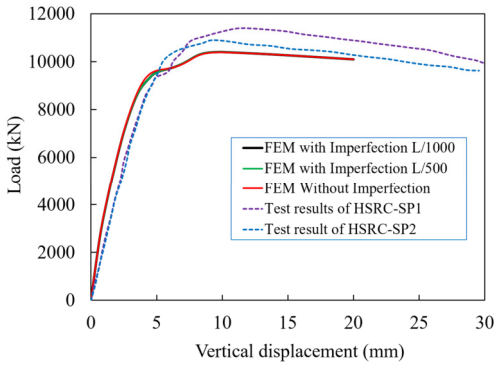

Fig. 5. Comparison of the L-D curves between FEM and the experimental results from [7].

TABLE III. COMPARISON OF THE ULTIMATE LOADS BETWEEN FEM AND THE EXPERIMENTAL RESULTS

Specimens	N_{Test} (kN)	N_{FEM1} (kN) (with imperfection)	N_{FEM2} (kN) (without imperfections)	N_{FEM1}/N_{Test}	N_{FEM2}/N_{Test}
HSRC-SP1	11363	10406	10393	0.92	0.91
HSRC-SP2	10890	10406	10393	0.96	0.95

Based on the FEM results, the stress state of the concrete of circular CESC columns in [7] is demonstrated in Figure 6. It can be observed from the stress in the 3-3 direction of the concrete that the I cross-shaped steel section provides a good confinement effect to the concrete. The stress concentration of the concrete inside the steel section is maximal at both ends and decreases to the middle of the column. A highly confined concrete zone is observed as seen in Figure 6. This zone is enclosed by steel web and flanges. This result is in line with the FEM result reported in [8].

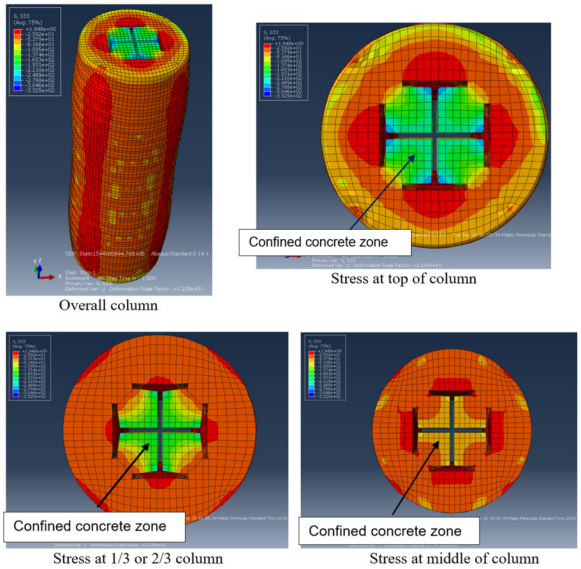

Fig. 6. Stresses in the concrete and the confined concrete zone.

IV. PARAMETRIC STUDY

The verified FEM was adopted for the parametric study to determine the effect of f_c, f_y, and s on the *L-D* curves of circular CESC short columns. All columns for the parametric study have the same diameter of 270mm and the same height of 800mm (L/D = 2.96). A steel section of 70×140×10×12 was chosen for the I-cross shape. The grade of the steel section is S355. The diameter of longitudinal reinforcement is d13 with a S500 grade. The diameter of spiral hoops is d10 with a S500 grade. Various concrete strengths (30, 100, 150MPa) and steel yield strengths (350, 550, and 650MPa) were modeled. The spacing of spiral hoops was taken as 30, 60, and 90mm. Eight longitudinal reinforcements were constructed for the columns. Figure 7 describes the circular CESC columns for the parametric study.

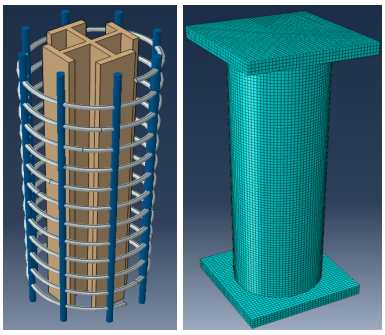

Fig. 7. The circular CESC columns for the parametric study.

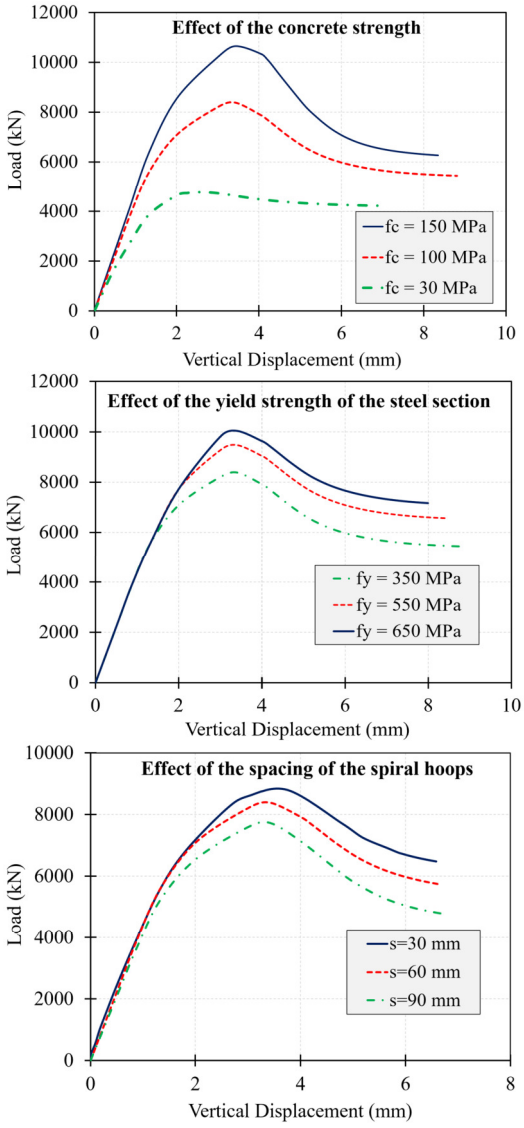

Fig. 8. Results of the parametric study using the verified FEM.

The results of the parametric study are illustrated in Figure 8. As expected, higher values of f_c and f_y result in higher composite column strength. When increasing f_c from 30 to 100MPa and from 30 to 150MPa, the loading capacity of the column was improved by about 76% and 123%, respectively.

The descending stage of the *L-D* curves of the columns using higher values of f_c was steeper than that when using lower values of f_c. When increasing f_y from 350 to 550MPa and from 350 to 650MPa, the strength enhancement of the CESC columns was about 13% and 19.7%, respectively. Unlike the effect of f_c, there was no significant improvement in the ductility of the columns with increasing yield strength f_y. Similar to the effect of f_y, smaller spacing of spiral hoops leads to higher column strength. Increasing the spacing of spiral hoops from 30 to 60mm and from 30 to 90mm decreased the column strength by about 4.7% and 7.8%, respectively. The quantitative value of strength improvement with increasing concrete strength f_c was higher than that with increasing f_y or decreasing s. There is no significant difference in the slope of the descending stage of the *L-D* curve with changes in f_y and s.

V. CONCLUSIONS

Deriving from the numerical results and analysis, the following conclusions can be indicated:

- The FEM results agreed well with the test results in [7]. Therefore the established FEM is reliably adopted to analyze the compressive behavior of circular CESC stub columns.
- Distribution of the stresses on the cross-section at different column heights was observed in the FEM results. A highly confined concrete zone can be observed in FEM. This zone is enclosed by steel web and steel flanges.
- Increased concrete strength, steel yield strength and decreasing spacing of spiral hoops, improve column strength.
- The shape of the descending branch in the *L-D* curves and the strength enhancement are significantly affected by the changes in concrete strength.

REFERENCES

[1] C. C. Chen and S. C. Yeh, "Ultimate strength of concrete encased steel composite columns," in *Proceedings of the third national conference on structural engineering*, pp. 2197-2206, 1996.

[2] S. El-Tawil and G. G. Deierlein, "Strength and Ductility of Concrete Encased Composite Columns," *Journal of Structural Engineering*, vol. 125, no. 9, pp. 1009–1019, Sep. 1999, https://doi.org/10.1061/(ASCE)0733-9445(1999)125:9(1009).

[3] C.-C. Chen and N.-J. Lin, "Analytical model for predicting axial capacity and behavior of concrete encased steel composite stub columns," *Journal of Constructional Steel Research*, vol. 62, no. 5, pp. 424–433, May 2006, https://doi.org/10.1016/j.jcsr.2005.04.021.

[4] E. Ellobody and B. Young, "Numerical simulation of concrete encased steel composite columns," *Journal of Constructional Steel Research*, vol. 67, no. 2, pp. 211–222, Feb. 2011, https://doi.org/10.1016/j.jcsr.2010.08.003.

[5] C.-S. Kim, H.-G. Park, K.-S. Chung, and I.-R. Choi, "Eccentric Axial Load Testing for Concrete-Encased Steel Columns Using 800 MPa Steel and 100 MPa Concrete," *Journal of Structural Engineering*, vol. 138, no. 8, pp. 1019–1031, Aug. 2012, https://doi.org/10.1061/(ASCE)ST.1943-541X.0000533.

[6] W.-Q. Zhu, G. Meng, and J.-Q. Jia, "Experimental studies on axial load performance of high-strength concrete short columns," *Proceedings of the Institution of Civil Engineers - Structures and Buildings*, vol. 167, no. 9, pp. 509–519, Sep. 2014, https://doi.org/10.1680/stbu.13.00027.

[7] S. W. Chen, P. Wu, Q. Liu, Z. X. Hou, and L. N. Qiu, "Studies on axially compressed SRC column using Q460 high strength steel," in *The 8th International Conference on Behavior of Steel structures in Seismic Area*, 2015.

[8] S. Chen and P. Wu, "Analytical model for predicting axial compressive behavior of steel reinforced concrete column," *Journal of Constructional Steel Research*, vol. 128, pp. 649–660, Jan. 2017, https://doi.org/10.1016/j.jcsr.2016.10.001.

[9] S.-P. Chiew and Y.-Q. Cai, "Design of high-strength steel reinforced concrete columns – a Eurocode 4 approach," *Steel Construction*, vol. 11, no. 4, pp. 306–314, 2018, https://doi.org/10.1002/stco.201800020.

[10] P. Lacki, A. Derlatka, and P. Kasza, "Comparison of steel-concrete composite column and steel column," *Composite Structures*, vol. 202, pp. 82–88, Oct. 2018, https://doi.org/10.1016/j.compstruct.2017.11.055.

[11] W. Anuntasena, A. Lenwari, and T. Thepchatri, "Finite Element Modelling of Concrete-Encased Steel Columns Subjected to Eccentric Loadings," *Engineering Journal*, vol. 23, no. 6, pp. 299–310, Nov. 2019, https://doi.org/10.4186/ej.2019.23.6.299.

[12] F. R. Kurniawan and Z. Al Jauhari, "Parametric study of CES composite columns with FRC using finite element analysis," *International Journal of GEOMATE*, vol. 16, no. 58, pp. 171–177, Dec. 2021, https://doi.org/10.21660/2019.58.8299.

[13] B. Lai, J. Y. R. Liew, and A. L. Hoang, "Behavior of high strength concrete encased steel composite stub columns with C130 concrete and S690 steel," *Engineering Structures*, vol. 200, Dec. 2019, Art. no. 109743, https://doi.org/10.1016/j.engstruct.2019.109743.

[14] B. Lai, J. Y. R. Liew, and M. Xiong, "Experimental study on high strength concrete encased steel composite short columns," *Construction and Building Materials*, vol. 228, Dec. 2019, Art. no. 116640, https://doi.org/10.1016/j.conbuildmat.2019.08.021.

[15] B. Lai, J. Y. Richard Liew, and T. Wang, "Buckling behaviour of high strength concrete encased steel composite columns," *Journal of Constructional Steel Research*, vol. 154, pp. 27–42, Mar. 2019, https://doi.org/10.1016/j.jcsr.2018.11.023.

[16] L. Sun *et al.*, "Experimental investigation on axial compression behavior of steel reinforced concrete columns with welded stirrups," *Engineering Structures*, vol. 208, Apr. 2020, Art. no. 109924, https://doi.org/10.1016/j.engstruct.2019.109924.

[17] T. Kartheek and T. Venkat Das, "3D modelling and analysis of encased steel-concrete composite column using ABAQUS," *Materials Today: Proceedings*, vol. 27, pp. 1545–1554, Jan. 2020, https://doi.org/10.1016/j.matpr.2020.03.200.

[18] P. C. Nguyen, D. D. Pham, T. T. Tran, and T. Nghia-Nguyen, "Modified Numerical Modeling of Axially Loaded Concrete-Filled Steel Circular-Tube Columns," *Engineering, Technology & Applied Science Research*, vol. 11, no. 3, pp. 7094–7099, Jun. 2021, https://doi.org/10.48084/etasr.4157.

[19] A. N. Hassooni and S. R. A. Zaidee, "Behavior and Strength of Composite Columns under the Impact of Uniaxial Compression Loading," *Engineering, Technology & Applied Science Research*, vol. 12, no. 4, pp. 8843–8849, Aug. 2022, https://doi.org/10.48084/etasr.4753.

[20] Z. H. Abdulghafoor and H. A. Al-Baghdadi, "Static and Dynamic Behavior of Circularized Reinforced Concrete Columns Strengthened with Hybrid CFRP," *Engineering, Technology & Applied Science Research*, vol. 12, no. 5, pp. 9336–9341, Oct. 2022, https://doi.org/10.48084/etasr.5162.

[21] *Abaqus/CAE User's Manual, version 6.8-1*. Hibbitt. Karlsson and Sorensen, Inc., 2015.

[22] M. Pagoulatou, T. Sheehan, X. H. Dai, and D. Lam, "Finite element analysis on the capacity of circular concrete-filled double-skin steel tubular (CFDST) stub columns," *Engineering Structures*, vol. 72, pp. 102–112, Aug. 2014, https://doi.org/10.1016/j.engstruct.2014.04.039.

[23] *CEB, High performance concrete recommended extensions to the model code 90 research needs. Lausanne, Switzerland: Comite Euro-International du Beton, 1995.*

[24] A. Venkateshwaran, B.-L. Lai, and J. Y. R. Liew, "Buckling resistance of steel fibre-reinforced concrete encased steel composite columns,"

Journal of Constructional Steel Research, vol. 190, Mar. 2022, Art. no. 107140, https://doi.org/10.1016/j.jcsr.2022.107140.

[25] K.-S. Park, S.-S. Lee, K.-W. Bae, and J. Moon, "Strength of Partially Encased Steel-Concrete Composite Column for Modular Building Structures," *Materials*, vol. 15, no. 17, Jan. 2022, Art. no. 6045, https://doi.org/10.3390/ma15176045.

[26] C.-C. Chen, C.-C. Chen, and K.-S. Zhan, "Design of confinement reinforcement for encased composite columns," *Engineering Structures*, vol. 250, Jan. 2022, Art. no. 113342, https://doi.org/10.1016/j.engstruct. 2021.113342.

[27] M. Naghipour, M. Ahmadi, and M. Nematzadeh, "Effect of concrete confinement level on load-bearing capacity of steel-reinforced concrete (SRC) columns under eccentric loading: Experiment and FEA model," *Structures*, vol. 35, pp. 202–213, Jan. 2022, https://doi.org/10.1016/ j.istruc.2021.10.094.

[28] M. K. I. Khan, C. K. Lee, Y. X. Zhang, and M. M. Rana, "Finite element analysis of engineered cementitious composite (ECC)-concrete-encased steel composite columns under axial compression," in *Advances in Engineered Cementitious Composites*, Y. X. Zhang and K. Yu, Eds. Pittsburgh, PA, USA: Woodhead Publishing, 2022, pp. 501–530.

[29] A. Elbably, O. Ramadan, A. Akl, and N. Zenhom, "Behavior of encased steel-high strength concrete columns against axial and cyclic loading," *Journal of Constructional Steel Research*, vol. 191, Apr. 2022, Art. no. 107161, https://doi.org/10.1016/j.jcsr.2022.107161.

[30] C. S. Reshma, C. P. Sudha, and P. Seena, "Experimental and Numerical Analysis of Axial Load Capacity of Encased Steel–concrete Composite Column," in *International Conference on Structural Engineering and Construction Management*, Dec. 2021, pp. 1115–1125, https://doi.org/ 10.1007/978-3-030-80312-4_97.